Published OnlineFirst October 25, 2011; DOI: 10.1158/1535-7163.MCT-11-0341

Molecular Cancer Therapeutics

Preclinical Development

A Polymeric Nanoparticle Encapsulated Small-Molecule Inhibitor of Hedgehog Signaling (NanoHHI) Bypasses Secondary Mutational Resistance to Smoothened Antagonists

Venugopal Chenna[1], Chaoxin Hu[1], Dipankar Pramanik[1], Blake T. Aftab[2], Collins Karikari[1], Nathaniel R. Campbell[1], Seung-Mo Hong[1], Ming Zhao[2], Michelle A. Rudek[2], Saeed R. Khan[2,3], Charles M. Rudin[2], and Anirban Maitra[1,2]

Abstract

Aberrant activation of the hedgehog (Hh) signaling pathway is one of the most prevalent abnormalities in human cancer. Tumors with cell autonomous Hh activation (e.g., medulloblastomas) can acquire secondary mutations at the Smoothened (Smo) antagonist binding pocket, which render them refractory to conventional Hh inhibitors. A class of Hh pathway inhibitors (HPI) has been identified that block signaling downstream of Smo; one of these compounds, HPI-1, is a potent antagonist of the Hh transcription factor Gli1 and functions independent of upstream components in the pathway. Systemic administration of HPI-1 is challenging due to its minimal aqueous solubility and poor bioavailability. We engineered a polymeric nanoparticle from [poly (lactic-co-glycolic acid); (PLGA)] conjugated with polyethylene glycol (PEG), encapsulating HPI-1 (NanoHHI). NanoHHI particles have an average diameter of approximately 60 nm, forms uniform aqueous suspension, and improved systemic bioavailability compared with the parent compound. In contrast to the prototype targeted Smo antagonist, HhAntag (Genentech), NanoHHI markedly inhibits the growth of allografts derived from $Ptch^{-/+}$; $Trp53^{-/-}$ mouse medulloblastomas that harbor a Smo^{D477G} binding site mutation ($P < 0.001$), which is accompanied by significant downregulation of m*Gli1* as well as bona fide Hh target genes (*Akna*, *Cltb*, and *Olig2*). Notably, NanoHHI combined with gemcitabine also significantly impedes the growth of orthotopic Pa03C pancreatic cancer xenografts that have a ligand-dependent, paracrine mechanism of Hh activation when compared with gemcitabine alone. No demonstrable hematologic or biochemical abnormalities were observed with NanoHHI administration. NanoHHI should be amenable to clinical translation in settings where tumors acquire mutational resistance to current Smo antagonists. *Mol Cancer Ther; 11(1); 165–73. ©2011 AACR.*

Introduction

The Hedgehog (Hh) signaling pathway plays a critical role in development as well as in mature tissue homeostasis (1). Aberrant activation of the Hh pathway is commonly observed in many human cancers, and it is implicated in tumor initiation as well as tumor progression (2, 3). Hh activation in human cancers can occur either via a ligand-independent mechanism, as is observed in so-called Gorlin syndrome cancers (basal cell carcinoma and medulloblastoma), or by a ligand-dependent mechanism, which has been implicated in many solid tumors (4, 5). Ligand-independent pathway activation is usually a consequence of loss-of-function mutations in the gene encoding the Hh inhibitory receptor Patched (Ptch), or less commonly, a gain-of-function mutation in the gene encoding the essential Hh signal transduction receptor Smoothened (Smo; refs. 6–8). In contrast, mutational activation of the pathway is rare in endodermal tumors such as pancreatic cancer that produce aberrantly high levels of Hh ligand (2). As recent evidence has shown, most of the pathway activity in such cancers seems to be restricted to the juxtatumoral stromal cells rather than the neoplastic cells per se (9, 10). Irrespective of the mechanism of pathway activation, derepression of Smo from Ptch initiates an intracellular cascade that culminates in the nuclear translocation of Gli transcription factors, and the major

Authors' Affiliations: Departments of [1]Pathology and [2]Oncology, The Sol Goldman Pancreatic Cancer Research Center, Johns Hopkins University School of Medicine, Baltimore; and [3]Food and Drug Administration Center for Drug Evaluation and Research, Silver Spring, Maryland

Note: Supplementary material for this article is available at Molecular Cancer Therapeutics Online (http://mct.aacrjournals.org/).

Note: V. Chenna and C. Hu contributed equally to this work.

Corresponding Author: Anirban Maitra, The Sol Goldman Pancreatic Cancer Research Center, Room 345, CRB-II, Johns Hopkins University School of Medicine, 1550 Orleans St, Baltimore, MD 21231. Phone: 410-955-3511; Fax: 410-614-0671; E-mail: amaitra1@jhmi.edu

doi: 10.1158/1535-7163.MCT-11-0341

Published OnlineFirst October 25, 2011; DOI: 10.1158/1535-7163.MCT-11-0341

transcriptional activator in human cancers seems to be Gli1, a product of the *GLI1* oncogene (11).

In the area of clinical oncology, small-molecule antagonists of Hh signaling have emerged as a more promising targeted approach to cancer therapy. Recently, there has been compelling evidence to suggest that cancer cells can acquire resistance to Smo antagonists through secondary mutations in *Smo*. Most notably, Yauch and colleagues recently reported on a patient with metastatic medulloblastoma, who initially had a dramatic response to GDC-0449, but subsequently relapsed with refractory disease (12). Sequencing of the relapsed tumor DNA identified a secondary mutation in an extracellular loop of the Smo heptahelical bundle (Smo^{D473H}), which abrogates the binding of GDC-0449. Strikingly, in a $Ptch^{-/+}$; $p53^{-/-}$ mouse model of medulloblastoma selected *in vivo* for resistance to GDC-0449, an acquired Smo^{D477G} alteration was identified, which is orthologous to the aspartic acid residue at position 473 in humans and similarly disrupts antagonist binding. Of note, neither mutation has an impact on the overall level of Hh activation, suggesting that these are not independently oncogenic. Independent experiments in murine medulloblastoma models have also reported comparable acquired mutations in *Smo* that confer Hh inhibitor resistance (13, 14). In addition, other mechanisms of resistance to Smo antagonists have also been reported, including amplification of *Gli* oncogenes that occur downstream of the Smo receptor (13, 14), thus allowing cancer cells to bypass Hh blockade by the current compendium of Smo antagonists.

In light of this emerging evidence on mechanisms of secondary resistance to Smo antagonists, there is a pressing need to identify a new generation of Hh inhibitors that block signaling downstream of Smo. In 2009, Hyman and colleagues identified a series of 4 Hh pathway inhibitors (HPI 1–4), which block signaling at diverse points downstream of Smo, including Gli processing, stability, and trafficking to the primary cilium (15). One of these compounds, HPI-1, is a potent antagonist of both endogenous activator Gli proteins (Gli1/2) and can also abrogate Hh signaling in the setting of exogenous Gli overexpression. On the basis of its mechanism of action, we can postulate that HPI-1 will circumvent acquired mutational resistance to conventional Smo inhibitors.

Despite the promising *in vitro* findings, however, the *in vivo* translation of HPI-1 is likely to be hampered by its highly lipophilic nature and poor aqueous solubility, thereby impairing systemic bioavailability. To harness the full therapeutic potential of HPI-1, we have generated a polymer nanoparticle-encapsulated formulation of HPI-1 (NanoHHI), which overcomes the barriers to systemic bioavailability. NanoHHI has been engineered using [poly(lactic-co-glycolic acid); (PLGA)] conjugated with polyethylene glycol (PEG), both of which are considered as generally regarded as safe components by the U.S. Food and Drug Administration (16). NanoHHI shows strikingly higher systemic bioavailability than the HPI-1 alone upon parenteral administration, with no apparent histopathologic or biochemical evidence of toxicities in mice. Of importance, NanoHHI blocks Hh signaling in cells with ectopic expression of the human Smo^{D473H} allele and significantly inhibits the *in vivo* growth of murine medulloblastoma allografts harboring the acquired murine Smo^{D477G} mutation, both of which confer resistance to targeted Smo antagonists (12). NanoHHI also inhibits the growth of orthotopic human pancreatic cancer xenografts that harbor a wild-type *Smo* allele, by potentiating the effects of gemcitabine in the orthotopic milieu. Thus, NanoHHI represents a promising new therapeutic formulation for treatment of human cancers with primary or secondary resistance to Smo antagonists.

Materials and Methods

Materials

PLGA conjugated with PEG, that is, PLGA-PEG (5050 DLG, mPEG 5000) was purchased from Lakeshore Biomaterials. Dichloromethane, acetone, and polyvinyl alcohol PVA_{18k} (87%–89% hydrolyzed) were obtained from Sigma Aldrich. HPI-1 was synthesized according to the reported procedure (15); the nanoparticulated formulation NanoHHI was stored as a lyophilized powder at 4°C and dissolved in PBS on the day of use. Gemcitabine (NetQem LLC) was stored at 4°C and dissolved in sterile NaCl (0.9% w/v) on the day of use. HhAntag (Genentech), a parental drug of the lead clinical compound GDC-0449 (17), was freshly formulated as a suspension in 0.5% methylcellulose/0.2% Tween-80 (MCT).

Cell lines and plasmids

Pa03C (LZ10.7), a low-passage metastatic human pancreatic cancer cell line, was cultured as described (18); the authentication of this cell line was based on representative validation of previously described whole exome mutational profiling data (19). Either wild-type *Smo* or Smo^{D473H} mutant cDNA was cloned into pRK5 mammalian expression vector, and stable clones of HEK293 cells expressing empty pRK5, pRK5-Smo^{wt}, or pRK5-Smo^{D473H} were generated for Hh reporter assays. Murine medulloblastoma allografts derived from $Ptch^{-/+}$; $p53^{-/-}$ mice harboring either Smo^{wt} or Smo^{D477G} alleles were generated as described previously for *in vivo* studies comparing HhAntag and NanoHHI (12).

Formulation of HPI-1–loaded PLGA-PEG nanoparticles (NanoHHI)

NanoHHI was prepared with a modification of the oil-in-water (o/w) emulsion solvent evaporation method (20). Briefly, 3 g of PLGA-PEG and 60 mg of HPI-1 was dissolved in 30 mL of dichloromethane and acetone (8:2), and the resulting solution was added to 0.4% polyvinyl alcohol (150 mL). The mixture was sonicated for 3 minutes with stirring (20W, 4°C). The suspension was stirred at room temperature for 4 hours to evaporate organic solvents, and complete evaporation of organic solvents was achieved by using the rotary evaporator. The resulting

Published OnlineFirst October 25, 2011; DOI: 10.1158/1535-7163.MCT-11-0341

suspension was ultracentrifuged at 40,000 rpm for 45 minutes. The precipitated nanoparticle pellet was washed 3 times with ultrapure water and resuspended in ultrapure water by mild sonication and centrifuged at 3,000 rpm for 5 minutes to remove large aggregates or any nonencapsulated drug. The supernatant NanoHHI was flash frozen on dry ice and lyophilized to obtain a dry NanoHHI powder amenable to long-term storage. Drug loading and loading efficiency were determined by dissolving dried NanoHHI in 80% methanol in water and quantifying by high-performance liquid chromatography (HPLC). Drug loading percentage (L) was calculated as follows: $L = (m_{drug}/m_{total}) \times 100$, where m_{drug} and m_{total} are the mass of drug and loaded nanoparticles (NanoHHI), respectively. Loading efficiency (E) was calculated as follows: $E = (m_{encap}/m_{drug}) \times 100$, where m_{encap} and m_{drug} are the mass of drug encapsulated and the total mass of drug initially loaded, respectively.

Size determination and *in vitro* release kinetics of NanoHHI

Size analysis of NanoHHI was done with a Malvern Zetasizer (Malvern), and transmission electron microscopy images obtained with a Hitachi 7600 (Hitachi Ltd.). Release kinetics studies were done with the dialysis method, as described (21). Briefly, NanoHHI containing 10 mg equivalent of HPI-1 dispersed in 5mL ultrapure water was transferred into a dialysis bag with a molecular cutoff value of 12 kDa. The bag was suspended in 100 mL of release medium [50% (v/v) of ethanol, water] in a container, with stirring at 50 rpm at 37°C. A 300 μL aliquot was withdrawn at predetermined time intervals and replaced with fresh release medium. Finally these samples were analyzed by HPLC with a Waters HPLC system. As HPI-1 is poorly soluble in water, ethanol was used in the release medium to ensure sink conditions.

Pharmacokinetic analyses of parenteral NanoHHI compared with free HPI-1 including brain distribution of NanoHHI

To compare the *in vivo* pharmacokinetics of NanoHHI versus free HPI-1, we conducted 3 independent studies, each via a different route of administration: First, for the i.p. route, 2 cohorts of 3 mice each were administered a single i.p. injection of either 25 mg/kg free HPI-1 suspended in corn oil or 25 mg/kg NanoHHI equivalent. Second, for the i.v. route, 2 cohorts of 4 mice each were administered either 30 mg/kg free HPI-1 in 40% ethanol or 30 mg/kg NanoHHI equivalent. Third, for the oral bioavailability study, 2 arms of 4 mice each were administered a single per oral dose of either 30 mg/kg free HPI-1 suspended in corn oil or 30 mg/kg NanoHHI, via oral gavage. Finally, to assess the ability of NanoHHI to cross the blood–brain barrier (BBB), 2 cohorts of 3 mice each were administered a single intravenous injection of 30 mg/kg NanoHHI (this study was done in replicate to collect terminal brain samples at 2 different time points following injection). All of the earlier studies were conducted using nontumor bearing CD1 mice. Blood samples (50 μL) were obtained from the mice at predetermined time intervals postinjection, with EDTA-coated Microvette CB300 capillary tubes (Braintree Scientific). The plasma was separated by centrifuging the blood samples at a speed of 1000 × *g* for 5 minutes. Brain samples were collected immediately following euthanasia at 10 and 30 minutes postinjection.

HPI-1 levels were estimated with liquid chromatography/tandem mass spectrometry (LC/MS-MS). Tissue homogenates were prepared at a concentration of 200 mg/mL in plasma before extraction. HPI-1 was extracted by acetonitrile:*n*-butyl chloride (1:4, v/v) and separated on a Waters X-Terra MS C_{18} (50 × 2.1 mm, 3.5 μm) column with acetonitrile/water mobile phase (80:20, v/v) containing 0.1% formic acid using isocratic flow at 0.15 mL/minute for 5 minutes. Plasma calibration curves were prepared over the range of 0.01 to 2 μg/mL or 0.06 to 12 μg/g, with a 1:1,000 dilution being accurately quantitated. Concentration–time data were evaluated using a noncompartmental approach with individual profiles (WinNonlin Professional, version 5.2 software; Pharsight Corporation).

Allograft and xenograft studies

All small animal experiments described conformed to the guidelines of the Animal Care and Use Committee of Johns Hopkins University. Mice were maintained in accordance with the guidelines of the American Association of Laboratory Animal Care.

Establishment and treatment of subcutaneous mouse medulloblastoma allografts

Flanks of 5 to 6 weeks old male athymic *nu/nu* mice (Harlan Laboratories) were injected with a single-cell suspension (2×10^6 cells) of either Smo^{WT}; $Ptch^{+/-}$; $Trp53^{-/-}$ or Smo^{D477G}; $Ptch^{+/-}$; $Trp53^{-/-}$ in a total volume of 200 μL PBS/Matrigel [BD Biosciences; 1:1 (v/v), prechilled to 4°C]. One week after the injection of tumor cells, subcutaneous tumor volumes (V) were measured with digital calipers (Fisher Scientific) and calculated using the formula as follows: $V = 1/2(ab^2)$, where a is the biggest and b is the smallest orthogonal tumor diameter. Mice with successfully engrafted. Smo^{WT} or Smo^{D477G} allografts were then randomized into 3 cohorts of 6 animals each and administered one the following regimens: (i) void PLGA-PEG nanoparticles, (ii) NanoHHI at a dose of 30 mg/kg i.p. twice daily, and (iii) HhAntag at a dose of 100 mg/kg orally, once daily. NanoHHI dosing of 30 mg/kg was chosen after multiple dose tolerance study (data not shown). The allografted mice were monitored daily for any signs of toxicity and behavioral abnormalities during the treatment. Tumor size and body weight were measured every other day. At the end of treatment, allografts were harvested and preserved for mRNA extraction and quantitative real-time PCR analysis of Hh gene targets.

Published OnlineFirst October 25, 2011; DOI: 10.1158/1535-7163.MCT-11-0341

Establishment and treatment of orthotopic Pa03C pancreatic cancer xenografts

The generation of orthotopic Pa03C human pancreatic cancer xenografts by surgical implantation in athymic mice has been described previously by our group (18). Three weeks after surgical orthotopic implantation, the presence of intrapancreatic primary tumors was confirmed by ultrasound scan (Vevo660; VisualSonics). Twenty-eight mice with demonstrable primary xenografts were then randomized into 4 cohorts, with 7 mice per arm, as follows: (i) void PLGA-PEG nanoparticles, (ii) NanoHHI at a dose of 30 mg/kg i.p. twice daily, (iii) gemcitabine at a dose of 20 mg/kg i.p. twice weekly, or (iv) the combination of NanoHHI (30 mg/kg i.p. twice daily) and gemcitabine (20 mg/kg i.p. twice weekly). Both agents were administered for a period of 4 weeks. At the end of therapy, primary tumors were carefully excised from the pancreas and weighed. Portions of treated xenografts were also preserved for mRNA extraction and qRT-PCR for Hh gene targets (primer sequences for human and mouse genes are readily available upon request).

Results

Physicochemical characterization and *in vitro* release kinetics of NanoHHI

Transmission electron microscopy (Fig. 1A) and dynamic light scattering studies (data not shown) confirmed that NanoHHI has an average diameter of 60 nm. In contrast to the extremely poor aqueous solubility of free HPI-1, NanoHHI was well dispersed to form a uniform suspension in aqueous media (Fig. 1B). HPI-1 was loaded efficiently in the void PLGA-PEG nanoparticles [2% (w/w) loading; 90% encapsulation efficiency]. The *in vitro* release kinetics of HPI-1 from NanoHHI was assessed over an approximately 4-week period by dialysis method, using 50% v/v ethanol as release medium to ensure sink conditions due to the nearly complete insolubility of free HPI-1 in aqueous media (Fig. 1C). A small burst release in the initial 24 hours was observed (cumulative ~30%), followed by a relatively slow release over 3 days (cumulative ~70%), with complete drug being released by day 25.

Pharmacokinetics of parenteral NanoHHI compared with free HPI-1 and brain distribution of NanoHHI

We compared the bioavailability of NanoHHI to free HPI-1 dissolved in corn oil, following administration of a single equivalent dose of either formulation through the i.p. route in nontumor-bearing mice (Fig. 1D). Relevant pharmacokinetic parameters, including C_{max}, T_{max}, and area under curve (AUC) are tabulated in Supplementary Table S1. There was an appreciable difference in the bioavailability of intraperitoneal HPI-1 between the free drug and nano formulation, with NanoHHI showing an $AUC_{0-\infty}$ value twice that of free HPI-1 in corn oil

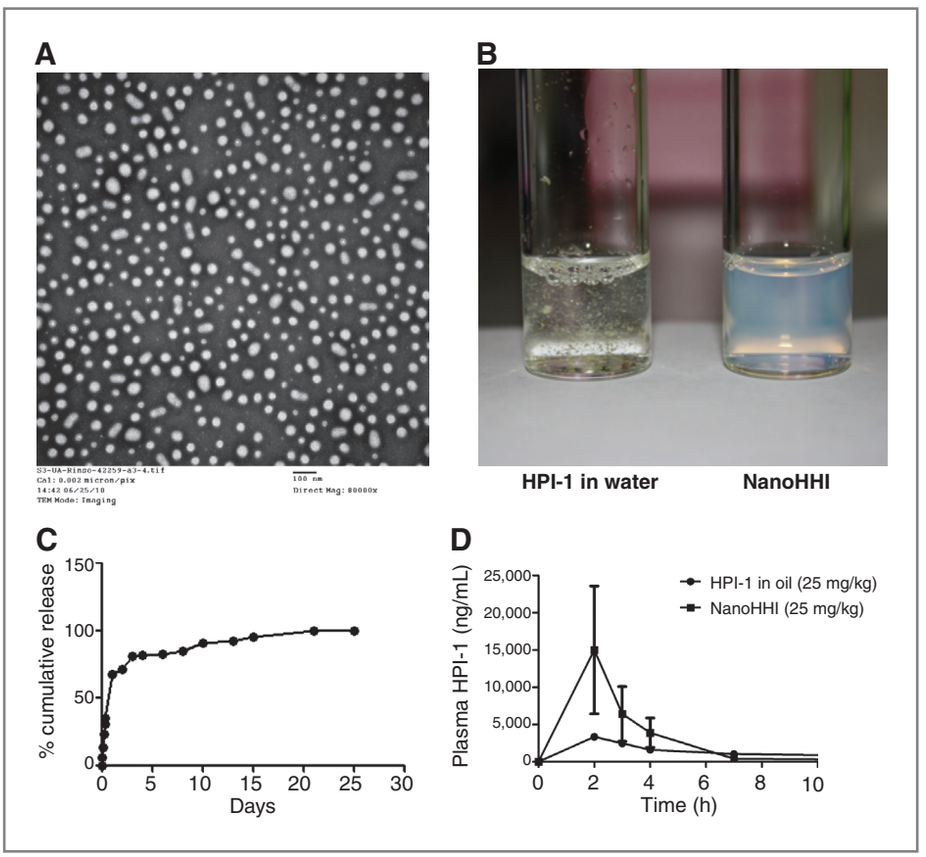

Figure 1. Physicochemical characterization and pharmacokinetics of NanoHHI. A, transmission electron micrograph pictures of NanoHHI, showing uniformly dispersed nanoparticles with an average size diameter of less than 100 nm. The scale bar on bottom right corner equals 100 nm. B, NanoHHI (right) is a uniform suspension in aqueous media, whereas parental HPI-1 is essentially insoluble, with flakes of drug clearly visible in the suspension. Equivalent amounts of HPI-1 were used in both instances. C, *in vitro* release kinetics of HPI-1 from NanoHHI, done at 37°C. The *y*-axis charts the percentage of cumulative release and the *x*-axis denotes time in days. D, pharmacokinetic disposition of parenteral NanoHHI administered as a single dose (25 mg/kg) compared with that of free HPI-1 (25 mg/kg) in corn oil. The experiments were done in nontumor-bearing CD1 mice, with 3 mice per cohort. Plasma HPI-1 levels were assessed with LC/MS-MS.

Published OnlineFirst October 25, 2011; DOI: 10.1158/1535-7163.MCT-11-0341

(52 ± 45 μg h/mL vs. 26 ± 12 μg h/mL). We also attempted to compare the pharmacokinetics of i.v. NanoHHI versus free HPI-1 dissolved in 40% ethanol as an excipient; however, the mice receiving intravenous ethanolic HPI-1 succumbed within 1 to 2 minutes of injection, likely from the excipient-related toxicity. The $AUC_{0-\infty}$ value of intravenous NanoHHI alone was 268 ± 98 μg h/mL (Supplementary Fig. S1A and Table S1). A more pronounced improvement in bioavailability was observed after oral administration of 30 mg/kg HPI-1 equivalents, with the NanoHHI $AUC_{0-\infty}$ value being 4-times higher than that of free HPI-1 in corn oil (17 ± 31 μg h/mL vs. 4.2 ± 1.4 μg h/mL; Supplementary Fig. S1B and Table S1). Thus, we were able to establish the feasibility of administering NanoHHI through multiple routes, with a 2- to 4-fold improved AUC values for the 2 modes (intraperitoneal and oral) where an equimolar comparison could be made versus free HPI-1.

A potential clinical application of Gli-targeted Hh agents will be in the setting of medulloblastomas that have acquired secondary mutations in *SMO*; thus, establishing tractable delivery of systemic NanoHHI past the BBB is paramount in that respect. Following single-dose intravenous administration of NanoHHI, HPI-1 was readily detectable in brain tissue at 3.9 ± 2.1 μg/g after 10 minutes and 1.4 ± 0.4 μg/g at 30 minutes after injection (Supplementary Fig. S1C).

NanoHHI inhibits the *in vivo* growth of murine medulloblastoma allografts harboring Smo antagonist–resistant binding site mutation

In vitro Hh reporter assays were conducted using HEK-293 cells expressing either wild-type pRK5-Smo^{WT} or the Smo antagonist–resistant binding site mutant pRK5-Smo^{D473H} construct (Fig. 2A). Whereas both HPI-1 and cyclopamine were able to significantly inhibit reporter activity in the setting of wild-type Smo, only HPI-1 resulted in significant downregulation of reporter activity in HEK-293 cells expressing the mutant Smo^{D473H}. These results confirmed the ability of our indigenously synthesized free HPI-1 to bypass the Smo binding site mutation *in vitro*.

We then proceeded to *in vivo* assays using the NanoHHI formulation, comparing it to the potent and selective Smo antagonist, HhAntag. In subcutaneous medulloblastoma allografts derived from Smo^{WT}; $Ptch^{+/-}$; $Trp53^{-/-}$ tumors, both NanoHHI and HhAntag inhibited *in vivo* growth to a comparable degree (Fig. 2B, left). In contrast, in allografts derived from Smo^{D477G}; $Ptch^{+/-}$; $Trp53^{-/-}$ tumors, there was a marked difference in efficacy between NanoHHI and HhAntag (Fig. 2B, right). Although even HhAntag had a significant negative impact on allograft growth ($P < 0.01$), NanoHHI essentially flattened the tumor growth curve ($P < 0.001$). The partial response seen with HhAntag in the setting of a binding site mutation may reflect residual binding capability to the mutant *Smo* receptor, and/or off-target effects, an effect not observed with the clinical grade compound (14). In treated allografts, qRT-PCR for Mm*Gli1* transcripts mirrored the efficacy data (Fig. 2C), with significant Mm*Gli1* downregulation observed in both treatment arms for Smo^{WT}; $Ptch^{+/-}$; $Trp53^{-/-}$ tumors ($P < 0.001$) but only in the NanoHHI arm for Smo^{D477G}; $Ptch^{+/-}$; $Trp53^{-/-}$ tumors ($P < 0.001$; all of the transcript results were normalized to levels observed in allografts treated with void polymer). Because HPI-1 is a direct inhibitor of Gli function and acts downstream of Smo, we evaluated the impact of NanoHHI or HhAntag treatment in a panel of recently described Gli target genes in murine medulloblastoma including *Akna*, *Cltb*, and *Olig2* (Fig. 2D; ref. 22). For these analyses, only the Smo^{D477G}; $Ptch^{+/-}$; $Trp53^{-/-}$ allografts were assessed, and confirmed the ability of NanoHHI, but not the targeted Smo inhibitor, to significantly block bona fide Gli target gene expression in the treated tumors. In this study, we observed no significant alterations of body weight in any of the NanoHHI treatment arms, whereas the HhAntag-treated mice showed approximately 10% body weight loss at the end of treatment (Supplementary Fig. S1D).

NanoHHI inhibits the growth of orthotopic pancreatic cancer xenografts in combination with gemcitabine

Gorlin syndrome tumors with cell autonomous Hh signaling comprise only a minor fraction of cases in the universe of solid cancers, with ligand-dependent Hh signaling being the most common mechanism of activation by far. In this latter instance, much of the signaling is paracrine in nature, and the nonneoplastic stromal cells may be significantly less likely to acquire secondary mutational hits during therapy. Nonetheless, given the demonstrable efficacy of Hh blockade in preclinical models of ligand-dependent cancers, we explored the *in vivo* effects of NanoHHI in an orthotopic human pancreatic cancer xenograft model. In Pa03C xenografts, we found that NanoHHI monotherapy had no significant effect on orthotopic tumor growth ($P = 0.58$), mirroring what has been reported with cyclopamine and other Smo antagonists (18, 23). In contrast, NanoHHI in combination with gemcitabine significantly improved tumor growth inhibition over gemcitabine alone ($P = 0.018$; Fig. 3A). We have previously shown that cyclopamine and other Smo antagonists deplete the primary tumor of cells expressing aldehyde dehydrogenase (ALDH), a credentialed marker of tumor-initiating cells (i.e., cancer stem cells; refs. 24, 25), even when there is no impact on gross tumor volume (18, 23). We confirmed that NanoHHI, either as a single agent, or in combination with gemcitabine, can cause a marked decrease in ALDH-expressing cells within the orthotopic Pa03C xenograft (Fig. 3B). Furthermore, we also confirmed that stroma-derived Mm*Gli1* was significantly reduced in both NanoHHI single-agent ($P < 0.05$) and combination therapy arms ($P < 0.001$; Fig. 3C), consistent with inhibition of Hh signaling in the murine stromal compartment. In contrast, gemcitabine alone had no significant impact on Mm*Gli1* levels. We also examined

Published OnlineFirst October 25, 2011; DOI: 10.1158/1535-7163.MCT-11-0341

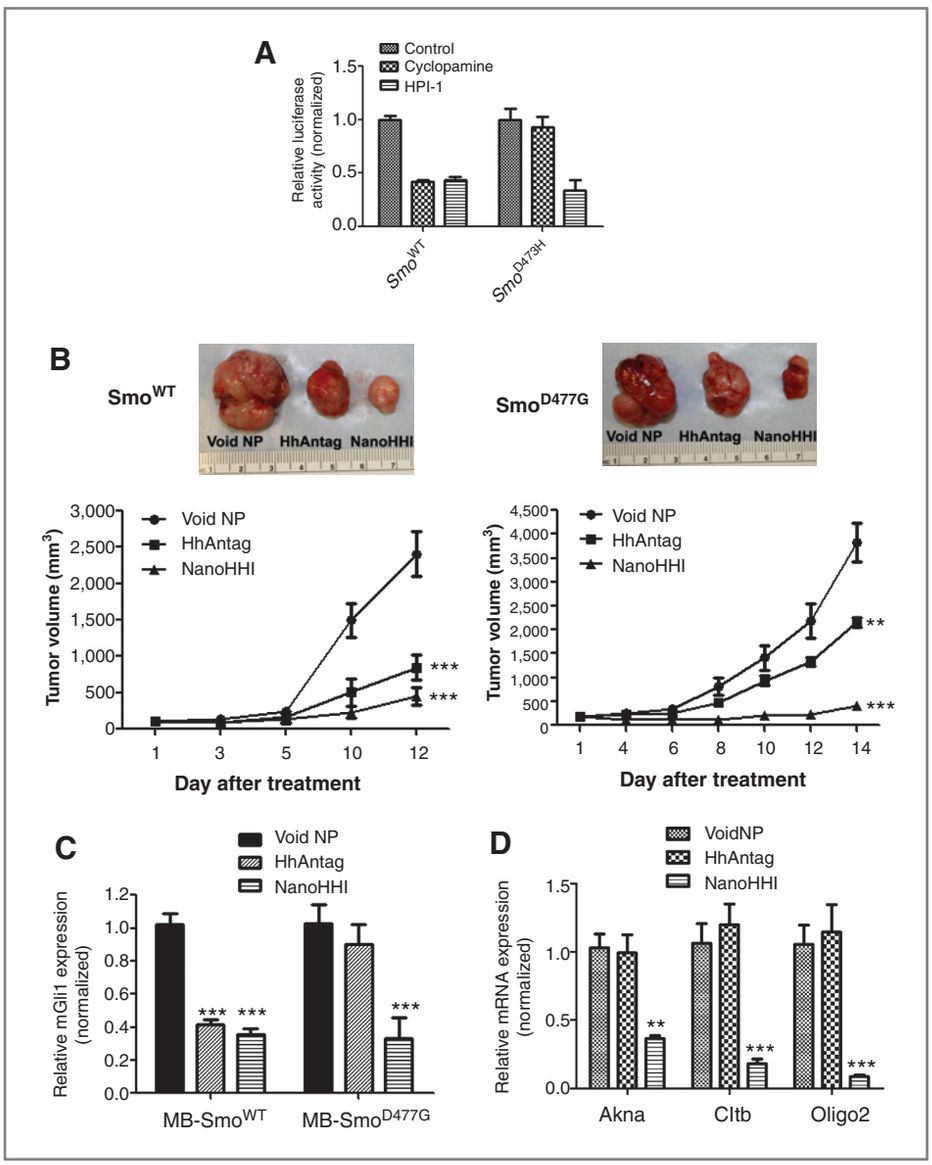

Figure 2. NanoHHI inhibits the *in vivo* growth of murine medulloblastoma allografts selected for acquired resistance to Smo inhibitors. A, HPI-1 can block Hh signaling in HEK-293 cells expressing human *Smo* (Hs*Smo*) with a binding site mutation. HEK-293 cells stably expressing either wild-type Hs*Smo* (*Smo*^{WT}) or mutant Hs*Smo*^{D473H} were transiently transfected with Gli1-binding site firefly luciferase reporter and exposed to cyclopamine or HPI-1. *Renilla* luciferase was used as a control for transfection efficiency. Both cyclopamine and HPI-1 can block Hh signaling in HEK-293 cells expressing Hs*Smo*^{WT} (left); in contrast, only HPI-1 blocks Hh signaling in HEK-293 cells expressing Hs*Smo*^{D473H}, whereas cyclopamine, which is unable to bind to mutant Smo receptor has minimal effect (right). All luciferase assays were done in triplicate, and the *y*-axis denotes relative luciferase units normalized to *Renilla*. B, murine medulloblastomas arising in *Ptch*$^{+/-}$; *Trp53*$^{-/-}$ mice and harboring either murine *Smo*^{WT} (Mm*Smo*^{WT}) or an acquired Mm*Smo*^{D477G} mutation were allografted subcutaneously in athymic mice and treated with either HhAntag or NanoHHI. Void PLGA-PEG nanoparticles (NP) were used as vehicle control. In allografts expressing wild-type Mm*Smo*, both HhAntag and NanoHHI show comparable effects in terms of tumor growth inhibition on day 12 (the experiment had to be terminated because of the rapid increase in growth of vehicle control allografts; left). In contrast, in allografts expressing the Mm*Smo*^{D477G} binding site mutation, NanoHHI shows a markedly better efficacy than HhAntag in growth inhibition (right, $P < 0.01$ for HhAntag and $P < 0.001$ for NanoHHI). Representative posttreatment allografts are shown above the growth plots for Smo^{WT} (top) and Smo^{D477G} (bottom), respectively. C, murine *Gli1* (Mm*Gli1*) mRNA levels were assessed following treatment in both cohorts as a measure of Hh pathway inhibition. Mirroring the growth phenotypes, both HhAntag and NanoHHI significantly downregulate Mm*Gli1* levels in Mm*Smo*^{WT} allografts, whereas only NanoHHI significantly downregulates Mm*Gli1* expression in Mm*Smo*^{D477G}-expressing allografts. The *y*-axis represents relative expression normalized to housekeeping control. D, in medulloblastoma allografts expressing the Mm*Smo*^{D477G} mutation, NanoHHI significantly downregulates bona fide Gli1 target genes, including *Akna*, *CItb*, and *Olig2*, compared with HhAntag-treated allografts (expression is normalized to the void polymer control treatment arm).

Published OnlineFirst October 25, 2011; DOI: 10.1158/1535-7163.MCT-11-0341

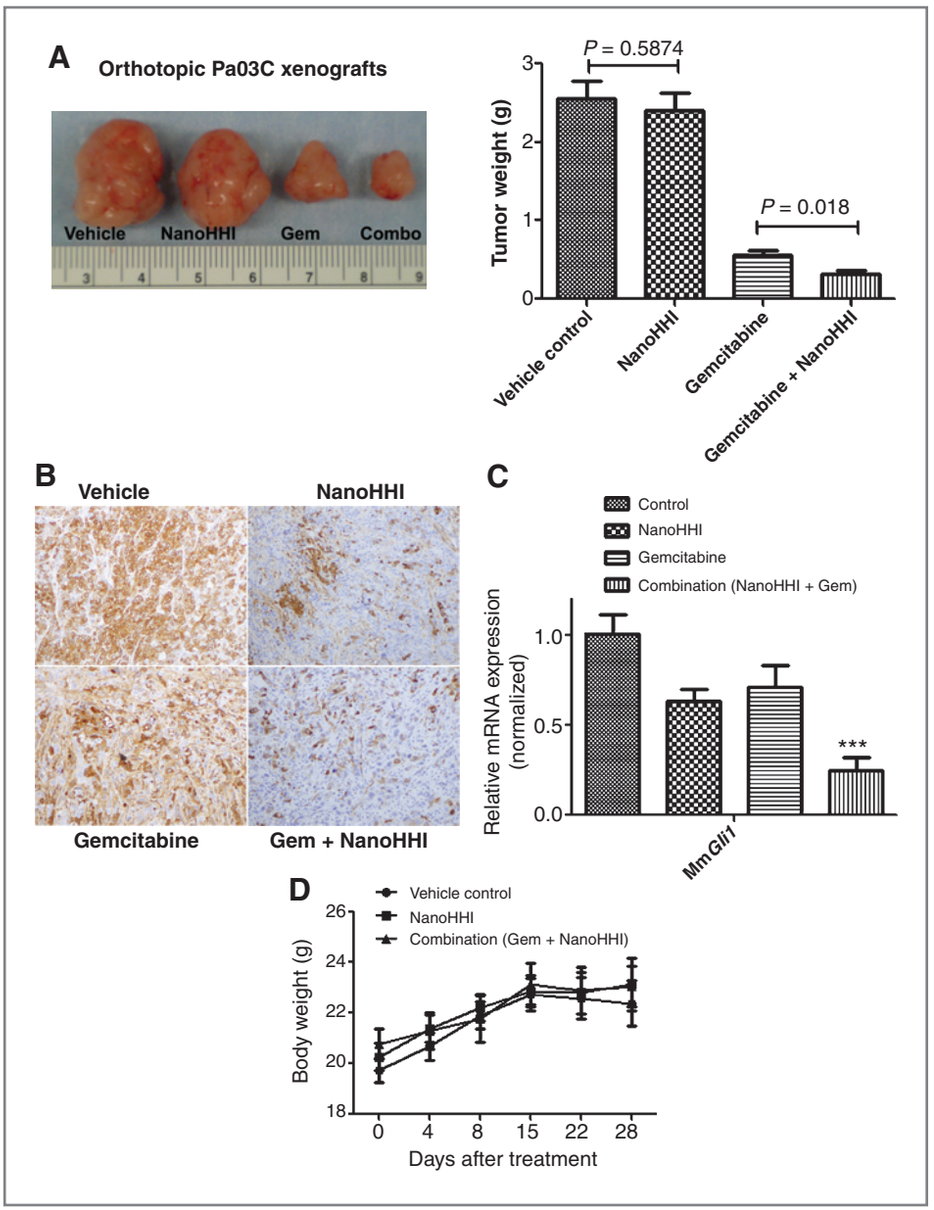

Figure 3. NanoHHI and gemcitabine blocks the growth of orthotopic pancreatic cancer xenografts with paracrine Hh signaling. A, orthotopic human pancreatic cancer Pa03C xenografts were generated in athymic mice by surgical orthotopic implantation and treated with vehicle control, NanoHHI, gemcitabine (Gem), or the combination (Combo). At 4 weeks of therapy, tumor weights were assessed at necropsy and showed a significant reduction in weight (in grams) for the combination arm compared with gemcitabine alone ($P = 0.018$). Expectedly, NanoHHI monotherapy had minimal impact on primary tumor weight. Representative posttreatment xenografts are shown for each cohort (left). B, NanoHHI depletes ALDH-expressing cells in Pa03C xenografts. ALDH expression in neoplastic cells was assessed by immunohistochemistry on representative xenografts from each of the 4 arms (as indicated). Marked reduction in ALDH-expressing cells is observed in both NanoHHI monotherapy and combination treatment arms. C, relative expression of stroma-specific murine *Gli1* (Mm*Gli1*) were assessed in the treated pancreatic cancer Pa03C xenografts. Significant downregulation of Mm*Gli1* was observed in both NanoHHI monotherapy ($P < 0.05$) and combination arms ($P < 0.001$), consistent with downregulation of Hh signaling in the stromal compartment. D, body weight measurements were obtained at 5 time points in mice bearing orthotopic Pa03C xenografts that were treated with vehicle, NanoHHI, or the combination of NanoHHI and gemcitabine over a 4-week time period. No significant body weight losses are encountered in either NanoHHI arm.

the levels of Hs*CMYC*, a key transcriptional regulator in pancreatic cancer, and found no significant effects of NanoHHI compared with void nanoparticles (notably, gemcitabine resulted in significant downregulation of expression in both single agent and combination therapy arms; Supplementary Fig. S2A). The expression of Hs*HES1*, a Notch pathway target gene, however, was significantly downregulated by NanoHHI, consistent with the recent data on noncanonical regulation of *HES1* expression by Hh signaling (26). Finally, we examined the

Published OnlineFirst October 25, 2011; DOI: 10.1158/1535-7163.MCT-11-0341

levels of Mm*Nestin*, a marker of neoendothelial cells in the murine stroma (27) and found significant downregulation in both single-agent and combination therapy arms, consistent with the known antiangiogenic effects of Hh blockade in tumors (Supplementary Fig. S2B).

Minimal systemic toxicity of NanoHHI in mice

The preclinical and emerging clinical use of the small-molecule Hh blockade has shown the surprising resilience of nonneoplastic Hh-dependent compartments (e.g., bone marrow) to this class of agents (28). Thus, there seems to be a therapeutic window, wherein depriving Hh signals to cancer cells themselves, or to the microenvironment, can inhibit tumor growth without major systemic deleterious effects. To determine whether a similar safety profile might exist for NanoHHI, particularly as the active pharmaceutical ingredient (API) has a distinct target (Gli) from the currently studied Smo antagonists, we did a panel of laboratory assays on NanoHHI-administered mice. In both the medulloblastoma allograft and the orthotopic pancreatic cancer xenograft experiments, which lasted for a period of 2 to 4 weeks, we observed no loss of body weight in any of the NanoHHI treatment arms (see Supplementary Fig. S1D and Fig. 3D). We also examined the histopathology of major viscera in NanoHHI-treated mice, which did not reveal any microscopic abnormalities (data not shown). Finally, we examined a panel of laboratory parameters, including hematologic (red blood cell, white blood cell, platelet counts, and hemoglobin), renal and liver function tests in NanoHHI mice compared with vehicle-treated animals (Supplementary Fig. S3) and observed no significant differences in any of the results.

Discussion

Aberrant activation of the Hh pathway is observed in many solid and hematologic cancers, generating considerable excitement about targeted inhibition of this pathway. As recent data have shown, patients whose tumors harbor mutational loss of *Patched* can experience dramatic responses to a class of orally bioavailable Smo antagonists, of which GDC-0449 is farthest along in clinical development (29, 30). Nonetheless, several mechanisms of secondary resistance to Hh blockade in tumors have emerged recently, most notably the acquisition of somatic mutations of *Smo*, which render the receptor incapable of binding to GDC-0449 and other antagonists of this class (12, 13). The acquisition of secondary resistance to targeted therapies is certainly not unprecedented, with chronic myelogenous leukemia being one of the better known examples where this phenomenon occurs in response to imatinib (31).

There is an urgent impetus for finding alternative targets in the Hh pathway, particularly those that function downstream of Smo. The Gli transcription factors represent ideal targets for this purpose, in light of their role as the final intracellular mediator of Hh signal transduction, both ligand dependent and independent. Given that *Gli1* can be either primarily amplified (e.g., in gliomas, from which this gene inherits its eponymous designation; ref. 32) or secondarily amplified/overexpressed in the setting of Hh inhibitor therapy (13), a pharmacologic strategy targeting Gli could have tangible benefits. Recent small molecule screens have indeed identified such lead candidates, of which a panel of 4 HPIs has been extensively characterized *in vitro* vis-à-vis their mechanisms of action (15). Of these, HPI-1 is a potent inhibitor of Gli function, including exogenously expressed *Gli1* in cells, underscoring its potential as an agent of choice in cancers that acquire resistance to Smo antagonists. A major pitfall of the parental HPI-1 compound is its lipophilicity, which makes systemic delivery and adequate bioavailability a challenge.

In this article, we present the initial characterization of a novel nanoparticle formulation of HPI-1 using the polymer PLGA as a backbone. PLGA has been extensively used as a vehicle for enabling systemic delivery of therapeutic agents that otherwise require noxious excipients like cremophor or ethanol and has been conferred a generally regarded as safe status by the U.S. Food and Drug Administration (16, 33). Although the active pharmaceutical ingredient in NanoHHI is identical to that of free HPI-1, we have showed the improved systemic bioavailability of the nanoformulation compared with the free drug upon both oral and parenteral administration in mice. In addition, we have documented the ability of intravenous NanoHHI to cross the BBB, resulting in detectable levels of the active pharmaceutical ingredient in the brain. In this study, we establish the ability of NanoHHI to bypass secondary resistance to conventional potent and selective Smo antagonists in a medulloblastoma allograft model. We have also shown that in preclinical models of pancreatic cancer, wherein the major component of Hh signaling is paracrine and acquired mutational resistance is potentially less of an issue, NanoHHI has therapeutic efficacy comparable with what has been reported for cyclopamine and related Smo antagonists (18, 23). Although we did not explicitly examine the efficacy of NanoHHI in a model of Gli overexpression (such as in a glioblastoma with *GLI1* amplification), data presented in the study by Hyman and colleagues suggest that NanoHHI should show activity in this setting, based on its ability to block Gli function at multiple levels (15). Whether NanoHHI also acts in acquired Smo inhibitor resistance secondary to other mechanisms like activation of the phosphoinositide 3-kinase pathway remains to be seen.

In conclusion, we present a novel polymer nanoparticle formulation of a potent Hh inhibitor, NanoHHI, which shows *in vivo* ability to circumvent acquired mutational resistance to the commonly used clinical Smo antagonists. In light of its demonstrable efficacy in preclinical allograft and xenograft models of both ligand-independent and

Published OnlineFirst October 25, 2011; DOI: 10.1158/1535-7163.MCT-11-0341

ligand-dependent Hh signaling and its ability to cross the BBB, NanoHHI has the potential to be used across a wide spectrum of tumor types. Future studies will expand the application of NanoHHI into the areas of autochthonous and orthotopic mouse models, including those generated by stereotactic injection within the central nervous system. The oral bioavailability of NanoHHI also provides an avenue for exploring a role for Hh-targeted chemoprevention in cognate systems.

Disclosure of Potential Conflicts of Interest

No potential conflicts of interest were disclosed.

The costs of publication of this article were defrayed in part by the payment of page charges. This article must therefore be hereby marked *advertisement* in accordance with 18 U.S.C. Section 1734 solely to indicate this fact.

Received May 9, 2011; revised September 17, 2011; accepted October 4, 2011; published OnlineFirst October 25, 2011.

References

1. Pasca di Magliano M, Hebrok M. Hedgehog signalling in cancer formation and maintenance. Nat Rev 2003;3:903–11.
2. Hidalgo M, Maitra A. The hedgehog pathway and pancreatic cancer. N Engl J Med 2009;361:2094–6.
3. Teglund S, Toftgard R. Hedgehog beyond medulloblastoma and basal cell carcinoma. Biochim Biophys Acta 2010;1805:181–208.
4. Watkins DN, Berman DM, Burkholder SG, Wang B, Beachy PA, Baylin SB. Hedgehog signalling within airway epithelial progenitors and in small-cell lung cancer. Nature 2003;422:313–7.
5. Berman DM, Karhadkar SS, Maitra A, Montes De Oca R, Gerstenblith MR, Briggs K, et al. Widespread requirement for Hedgehog ligand stimulation in growth of digestive tract tumours. Nature 2003;425:846–51.
6. Goodrich LV, Milenkovic L, Higgins KM, Scott MP. Altered neural cell fates and medulloblastoma in mouse patched mutants. Science 1997;277:1109–13.
7. Lam CW, Xie J, To KF, Ng HK, Lee KC, Yuen NW, et al. A frequent activated smoothened mutation in sporadic basal cell carcinomas. Oncogene 1999;18:833–6.
8. Dahmane N, Lee J, Robins P, Heller P, Ruiz i Altaba A. Activation of the transcription factor Gli1 and the Sonic hedgehog signalling pathway in skin tumours. Nature 1997;389:876–81.
9. Theunissen JW, de Sauvage FJ. Paracrine Hedgehog signaling in cancer. Cancer Res 2009;69:6007–10.
10. Yauch RL, Gould SE, Scales SJ, Tang T, Tian H, Ahn CP, et al. A paracrine requirement for hedgehog signalling in cancer. Nature 2008;455:406–10.
11. Ruiz i Altaba A, Mas C, Stecca B. The Gli code: an information nexus regulating cell fate, stemness and cancer. Trends Cell Biol 2007;17:438–47.
12. Yauch RL, Dijkgraaf GJ, Alicke B, Januario T, Ahn CP, Holcomb T, et al. Smoothened mutation confers resistance to a Hedgehog pathway inhibitor in medulloblastoma. Science 2009;326:572–4.
13. Buonamici S, Williams J, Morrissey M, Wang A, Guo R, Vattay A, et al. Interfering with resistance to smoothened antagonists by inhibition of the PI3K pathway in medulloblastoma. Sci Transl Med 2010;2:51ra70.
14. Dijkgraaf GJ, Alicke B, Weinmann L, Januario T, West K, Modrusan Z, et al. Small molecule inhibition of GDC-0449 refractory smoothened mutants and downstream mechanisms of drug resistance. Cancer Res 2011;71:435–44.
15. Hyman JM, Firestone AJ, Heine VM, Zhao Y, Ocasio CA, Han K, et al. Small-molecule inhibitors reveal multiple strategies for Hedgehog pathway blockade. Proc Natl Acad Sci U S A 2009;106:14132–7.
16. Lu JM, Wang X, Marin-Muller C, Wang H, Lin PH, Yao Q, et al. Current advances in research and clinical applications of PLGA-based nanotechnology. Expert Rev Mol Diagn 2009;9:325–41.
17. Romer JT, Kimura H, Magdaleno S, Sasai K, Fuller C, Baines H, et al. Suppression of the Shh pathway using a small molecule inhibitor eliminates medulloblastoma in Ptc1(+/−)p53(−/−) mice. Cancer Cell 2004;6:229–40.
18. Feldmann G, Dhara S, Fendrich V, Bedja D, Beaty R, Mullendore M, et al. Blockade of hedgehog signaling inhibits pancreatic cancer invasion and metastases: a new paradigm for combination therapy in solid cancers. Cancer Res 2007;67:2187–96.
19. Jones S, Zhang X, Parsons DW, Lin JC, Leary RJ, Angenendt P, et al. Core signaling pathways in human pancreatic cancers revealed by global genomic analyses. Science 2008;321:1801–6.
20. Gref R, Minamitake Y, Peracchia MT, Trubetskoy V, Torchilin V, Langer R. Biodegradable long-circulating polymeric nanospheres. Science 1994;263:1600–3.
21. Shaikh J, Ankola DD, Beniwal V, Singh D, Kumar MN. Nanoparticle encapsulation improves oral bioavailability of curcumin by at least 9-fold when compared to curcumin administered with piperine as absorption enhancer. Eur J Pharm Sci 2009;37:223–30.
22. Lee EY, Ji H, Ouyang Z, Zhou B, Ma W, Vokes SA, et al. Hedgehog pathway-regulated gene networks in cerebellum development and tumorigenesis. Proc Natl Acad Sci U S A 2011;107:9736–41.
23. Feldmann G, Fendrich V, McGovern K, Bedja D, Bisht S, Alvarez H, et al. An orally bioavailable small-molecule inhibitor of Hedgehog signaling inhibits tumor initiation and metastasis in pancreatic cancer. Mol Cancer Ther 2008;7:2725–35.
24. Jimeno A, Feldmann G, Suarez-Gauthier A, Rasheed Z, Solomon A, Zou GM, et al. A direct pancreatic cancer xenograft model as a platform for cancer stem cell therapeutic development. Mol Cancer Ther 2009;8:310–4.
25. Rasheed ZA, Yang J, Wang Q, Kowalski J, Freed I, Murter C, et al. Prognostic significance of tumorigenic cells with mesenchymal features in pancreatic adenocarcinoma. J Natl Cancer Inst 2010;102:340–51.
26. Ingram WJ, McCue KI, Tran TH, Hallahan AR, Wainwright BJ. Sonic Hedgehog regulates Hes1 through a novel mechanism that is independent of canonical Notch pathway signalling. Oncogene 2008;27:1489–500.
27. Teranishi N, Naito Z, Ishiwata T, Tanaka N, Furukawa K, Seya T, et al. Identification of neovasculature using nestin in colorectal cancer. Int J Oncol 2007;30:593–603.
28. Bisht S, Brossart P, Maitra A, Feldmann G. Agents targeting the Hedgehog pathway for pancreatic cancer treatment. Curr Opin Investig Drugs 2011;11:1387–98.
29. De Smaele E, Ferretti E, Gulino A. Vismodegib, a small-molecule inhibitor of the hedgehog pathway for the treatment of advanced cancers. Curr Opin Investig Drugs 2011;11:707–18.
30. Von Hoff DD, Lorusso PM, Rudin CM, Reddy JC, Yauch RL, Tibes R, et al. Inhibition of the hedgehog pathway in advanced Basal-cell carcinoma. N Engl J Med 2009;361:1164–72.
31. Gorre ME, Mohammed M, Ellwood K, Hsu N, Paquette R, Rao PN, et al. Clinical resistance to STI-571 cancer therapy caused by BCR-ABL gene mutation or amplification. Science 2001;293:876–80.
32. Kinzler KW, Bigner SH, Bigner DD, Trent JM, Law ML, O'Brien SJ, et al. Identification of an amplified, highly expressed gene in a human glioma. Science 1987;236:70–3.
33. Panyam J, Labhasetwar V. Biodegradable nanoparticles for drug and gene delivery to cells and tissue. Adv Drug Deliv Rev 2003;55:329–47.

Published OnlineFirst October 25, 2011; DOI: 10.1158/1535-7163.MCT-11-0341

Molecular Cancer Therapeutics

A Polymeric Nanoparticle Encapsulated Small-Molecule Inhibitor of Hedgehog Signaling (NanoHHI) Bypasses Secondary Mutational Resistance to Smoothened Antagonists

Venugopal Chenna, Chaoxin Hu, Dipankar Pramanik, et al.

Mol Cancer Ther 2012;11:165-173. Published OnlineFirst October 25, 2011.